

## Long-term performance assessment of nuclear waste and natural glasses in the geological repository: a geochemical modelling

Nishi Rani<sup>1</sup>, J. P. Shrivastava<sup>1\*</sup> and R. K. Bajpai<sup>2</sup>

<sup>1</sup>Department of Geology, University of Delhi, Delhi 110 007, India

<sup>2</sup>Nuclear Recycle Group, BARC, Mumbai 400 008, India

Nuclear waste loaded and natural (analogue) glasses were studied to understand neo-formed mineral species, formed in equilibrium with the physico-chemical conditions existing in the geological repository. To predict alteration-phases, dissolution equations for average vitrification system (AVS), barium borosilicate (BBS) and obsidian glass were calculated, considering glass composition, pressure, temperature and pH conditions. Progress of reaction plotted against saturation index, indicates saturation with solid phases – chamosite, chalcedony and Ca-beidellite in obsidian; greenalite and fayalite in AVS; and coffinite BBS glass. Activities and molalities of aqueous species together with the number of moles of each mineral species produced and degenerated during the progress of the reaction (as a function of time) are discussed in this communication.

**Keywords:** Geochemical modelling, geological repository, natural glass, nuclear waste.

NUCLEAR waste is stored in the form of glass in the geological repository. It provides long-term, safe isolation of radionuclide and toxic species from the environment. The process of vitrification involves assimilation of nuclear waste into high-silica glass, to develop a corrosion-resistant and highly durable matrix for its safe disposal in the geological repository. On disposal of the nuclear waste-loaded glass, it interacts with the geological environment and forms new mineral species which achieve equilibrium with the existing physico-chemical conditions. The processes which operate in this environment vary to a large extent when the pressure, temperature and nature of the fluids undergo changes. These parameters are interdependent; therefore, radionuclide behaviour cannot be assessed independently without the consideration of coprecipitation of other major or minor constituents in the system. Performance assessment of a glass in a geological repository is based on a series of calculation models applied to examine the consequences of matrix alteration by water and release of radionuclide into the environment. Therefore, the alteration mechanism must be quantified

by key parameters to assess the nuclear waste performance over a long term ( $10^6$  years<sup>1-3</sup>).

Mathematical expressions describe the theoretical concepts and thermodynamic relations on which the aqueous speciation, oxidation–reduction, precipitation–dissolution and adsorption–desorption calculations are based. These calculations are efficient as they encompass all the requisite sub-models and the imperative aqueous complexes, solids and gases for significant elements present. For a model with redox reactions, oxygen fugacity and pH are the logical choices as cations (e.g. Si, Al, Fe<sup>3+</sup>, Mg, Ca, Na and Na) and anions (e.g. H and OH) form the basis where species/minerals tend to associate with the charge balance equation. Application of geochemical codes for the performance assessment of nuclear waste and natural glasses has been reviewed<sup>4</sup>. It was concluded that the EQ3/6 (ref. 5) and GWB (ref. 6) codes are more pertinent for modelling aqueous speciation and reaction path. These codes also permit simulation of mass transfer due to mineral precipitation as a function of progress of the reaction. The simulated waste used in the present investigation represents its composition similar to the high level waste (HLW) to be processed. The Na<sub>2</sub>O–B<sub>2</sub>O<sub>3</sub>–SiO<sub>2</sub> ternary was used as a basic system for the selection of matrix composition. Computations were performed on average vitrification system (AVS) and barium borosilicate glasses (BBS), containing a complex mixture of simulated waste oxides. The base glass compositional ranges (SiO<sub>2</sub>: 35–40, B<sub>2</sub>O<sub>3</sub>: 20–25, Na<sub>2</sub>O: 2–15 and BaO: 2–25 wt%) were selected in accordance with the glass-forming region as marked over the SiO<sub>2</sub>–Na<sub>2</sub>O–B<sub>2</sub>O<sub>3</sub> ternary diagram demarcated in the SiO<sub>2</sub>–Na<sub>2</sub>O–B<sub>2</sub>O<sub>3</sub> ternary plot (Figure 1)<sup>7</sup>. These base glasses have been loaded with 15–30 wt% waste oxides (Table 1) to achieve waste

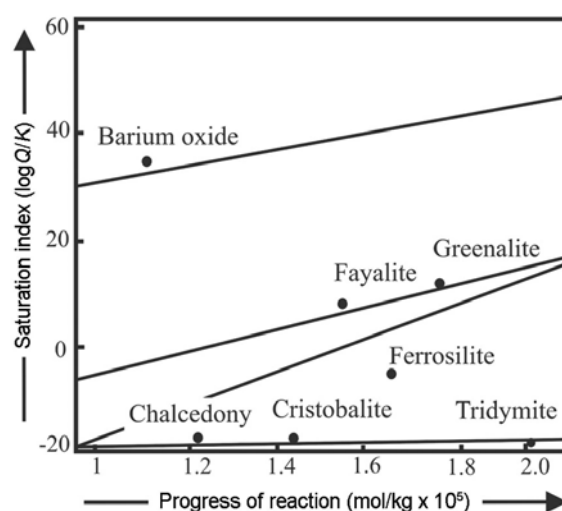


**Figure 1.** Data plots between progress of reaction and saturation index for average vitrification system (AVS) glass at 300°C in a nearly closed system indicating formation of aluminosilicate/silicate mineral phases.

\*For correspondence. (e-mail: jpshrivastava.du@gmail.com)

**Table 1.** Major oxides and waste oxides (in wt%) data for average vitrification system (AVS), barium borosilicate (BBS) and obsidian (natural analogue) glasses

| Oxides (wt%)                                | AVS glass* | Oxides (wt%)   | BBS glass <sup>#</sup> | Oxides (wt%)                                | Obsidian*<br>glass |
|---|------------|--|------------------------|---|--------------------|
| SiO <sub>2</sub>                            | 40.602     | SiO <sub>2</sub>                                     | 30.5                   | SiO <sub>2</sub>                            | 71.18              |
| B <sub>2</sub> O <sub>3</sub>               | 22.094     | B <sub>2</sub> O <sub>3</sub>                        | 20.0                   | TiO <sub>2</sub>                            | 00.36              |
| TiO <sub>2</sub>                            | 08.036     | Na <sub>2</sub> O                                    | 9.5                    | Al <sub>2</sub> O <sub>3</sub>              | 09.71              |
| Na <sub>2</sub> O                           | 20.832     | BaO  | 19.0                   | Fe <sub>2</sub> O <sub>3</sub> <sup>T</sup> | 05.26              |
| Fe <sub>2</sub> O <sub>3</sub> <sup>T</sup> | 05.536     | NaNO <sub>3</sub>                                    | 14.454                 | MnO   | 00.11              |
| K <sub>2</sub> O                            | 00.227     | U-solution   | 1.088                  | MgO   | 00.11              |
| CeO <sub>2</sub>                            | 01.286     | Al(NO <sub>3</sub> ) <sub>3</sub> ·9H <sub>2</sub> O | 2.829                  | CaO   | 01.96              |
| MnO   | 0.462      | Fe(NO <sub>3</sub> ) <sub>3</sub> ·9H <sub>2</sub> O | 1.247                  | Na <sub>2</sub> O                           | 05.51              |
| Cr <sub>2</sub> O <sub>3</sub>              | 0.193      | Ca(NO <sub>3</sub> ) <sub>2</sub> ·4H <sub>2</sub> O | 0.033                  | K <sub>2</sub> O                            | 00.03              |
| Cs <sub>2</sub> O                           | 0.178      | Ni(NO <sub>3</sub> ) <sub>2</sub> ·6H <sub>2</sub> O | 0.004                  | P <sub>2</sub> O <sub>5</sub>               | 05.76              |
| MoO <sub>3</sub>                            | 0.173      | CrO <sub>3</sub>                                     | 0.129                  |   |                    |
| BaO   | 0.060      | CsNO <sub>3</sub>                                    | 0.011                  |   |                    |
| SrO   | 0.206      | Sr(NO <sub>3</sub> ) <sub>2</sub>                    | 0.002                  |   |                    |
|   |            | Ce(NO <sub>3</sub> ) <sub>3</sub> ·6H <sub>2</sub> O | 0.017                  |   |                    |
|   |            | Nd <sub>2</sub> O <sub>3</sub>                       | 0.006                  |   |                    |
|   |            | RuO <sub>2</sub>                                     | 0.0024                 |   |                    |
|   |            | Na <sub>2</sub> SO <sub>4</sub>                      | 1.13                   |   |                    |
| Total                                       | 100        |  | 100                    |   | 100                |

\*Present data obtained by ICP fusion method; <sup>#</sup>Published values of Kaushik *et al.*<sup>17</sup>.

glass. The high radioactivity serves as a barrier for nuclear waste glass to be utilized in the laboratory. Therefore, for the present work, nuclear waste simulated (inactive) glass was prepared, which lacks radioactivity, but possesses a chemical composition close to HLW. For natural analogue major oxides were determined by ICP-MS fusion technique and when the chemical data were compared with the published obsidian compositions<sup>8</sup>, they showed a tight chemical closeness. These datasets when plotted in the total alkali–silica diagram, lie close to each other and fall in the rhyolite field<sup>5</sup>. Table 1 shows compositional datasets for AVS and BBS and obsidian glasses. In a natural volcanic silicate glass, SiO<sub>4</sub> tetrahedra are linked via bridging oxygen atoms at the vertices so that continuous three-dimensional networks are established. But, in case of nuclear waste-loaded B<sub>2</sub>O<sub>3</sub> glass system, the basic unit is triangular, where Si and B are the network formers (46–51 wt%) and are located at the centre of the oxygen polyhedra of the tetrahedra and triangles respectively<sup>9</sup>. The order of dissolution of the non-bridging species is somewhat more important than the bridging species of boric oxide, aluminium oxide and silica; thus Al and Si are the least mobilized and rate-limiting species. By the time their mobility commences, the radionuclide (e.g. Cs) and the associated non-bridging species (e.g. Na) migrate out of the glass, leaving behind a skeletal network of aluminum-silicate and mineral phases (e.g. smectite, saponite, illite, hydrocalcite and nontronite)<sup>10,11</sup>. Occurrence of alumino-silicate mineral phases in a repository indicates enrichment of radionuclides in an environment, far from the original *in situ* glass<sup>12</sup>. For the percentage of radionuclides retained in the alteration products<sup>13</sup>, Mn, Ti and Fe account for Ru,

Tc, Co and Rh; whereas Ni accounts for Pd, Pm, Sm and Eu. The behaviour of Ti, Mn and Ni serves as a simulating factor to ascertain the extent of glass alteration rate and its mechanism<sup>14</sup>.

In kinetic reaction paths, the rates at which minerals dissolve or precipitate are set by kinetic rate laws. The progress is measured in time, instead of non-dimensional variables. A mineral dissolves in a fluid up to saturation condition and precipitates when it is supersaturated. The formation of a pure solid phase is directly related to the speciation in the aqueous phase. The conversion of solid into liquid phase is accountable for the change in the solubility of the elements<sup>15</sup>. These geochemical codes predict dissolution rate of rapidly mobilizing species and their order of mobility. Owing to the dominance of rate-limiting species (e.g. silica >71 wt%) in obsidian glass, these codes have been used for the present mathematical calculations. But, relative intensities of bridging and non-bridging oxygen spectra are far apart in terms of structure, melting temperature, glass transition temperature and time–temperature-transformation. In this case the volcanic obsidian glass is considered as a reference material for comparison with the AVS and BBS glasses, because almost similar alumino-silicate mineral phases were yielded after alteration of fresh obsidian glass outcrop in the natural environment, since its formation ~66 Ma ago. Thus, for prediction of borosilicate waste glass dissolution rates by the current models, it is assumed that only the silica concentration of the solution affects the overall rate of the surface reaction<sup>16</sup>. The process is therefore modelled using affinity in terms of SiO<sub>2</sub> (aqueous) only. These models assume that the glass dissolution rates are exclusively a function of glass

**Table 2.** Speciation, activity constant, dissolution equation and saturation index calculated for AVS glass

| Species/minerals                             | Activity constant | Dissolution equation  | log <i>Q/K</i> |
|--|-------------------|---|----------------|
| SiO <sub>2</sub> (aq)                        | 40.64             | SiO <sub>2</sub> (aq) = SiO <sub>2</sub> (aq)   | 0.0000         |
| H <sub>3</sub> SiO <sub>4</sub> <sup>-</sup> | 40.64             | H <sub>3</sub> SiO <sub>4</sub> <sup>-</sup> + H <sup>+</sup> = SiO <sub>2</sub> (aq) + 2H <sub>2</sub> O             | 10.1769        |
| (BaO) <sub>2</sub> SiO <sub>2</sub>          | 1                 | (BaO) <sub>2</sub> SiO <sub>2</sub> + 4H <sup>+</sup> = SiO <sub>2</sub> (aq) + 2H <sub>2</sub> O + 2Ba <sup>++</sup> | 48.3812        |
| Amorphous silica                             | 1                 | Amorphous silica = SiO <sub>2</sub> (aq)  | -2.9906        |
| Chalcedony                                   | 1                 | Chalcedony = SiO <sub>2</sub> (aq)  | -4.2010        |
| Cristobalite                                 | 1                 | Cristobalite = SiO <sub>2</sub> (aq)  | -3.8866        |
| Fayalite                                     | 1                 | Fayalite + 4H <sup>+</sup> = SiO <sub>2</sub> (aq) + 2H <sub>2</sub> O + 2Fe <sup>++</sup>                            | 21.4988        |
| Ferrosilite                                  | 1                 | Ferrosilite + 2H <sup>+</sup> = SiO <sub>2</sub> (aq) + H <sub>2</sub> O + Fe <sup>++</sup>                           | 8.3598         |
| Greenalite                                   | 1                 | Greenalite + 6H <sup>+</sup> = 2SiO <sub>2</sub> (aq) + 5H <sub>2</sub> O + 3Fe <sup>++</sup>                         | 25.2665        |
| Na <sub>2</sub> SiO <sub>3</sub>             | 1                 | Na <sub>2</sub> SiO <sub>3</sub> + 2H <sup>+</sup> = SiO <sub>2</sub> (aq) + H <sub>2</sub> O + 2Na                   | 23.6470        |
| Quartz                                       | 1                 | Quartz = SiO <sub>2</sub> (aq)  | -4.4970        |
| Tridymite                                    | 1                 | Tridymite = SiO <sub>2</sub> (aq)   | -4.3059        |

**Table 3.** Speciation, activity constant, dissolution equation and saturation index calculated for BBS glass

| Species/minerals                             | Activity constant | Dissolution equation   | log <i>Q/K</i> |
|--|-------------------|--|----------------|
| SiO <sub>2</sub> (aq)                        | 40.64             | SiO <sub>2</sub> (aq) = SiO <sub>2</sub> (aq)  | 0.0000         |
| H <sub>3</sub> SiO <sub>4</sub> <sup>-</sup> | 14.32             | H <sub>3</sub> SiO <sub>4</sub> <sup>-</sup> + 2H <sup>+</sup> = SiO <sub>2</sub> (aq) + 2H <sub>2</sub> O             | 24.0746        |
| (BaO) <sub>2</sub> SiO <sub>2</sub>          | 1                 | (BaO) <sub>2</sub> SiO <sub>2</sub> + 4H <sup>+</sup> = SiO <sub>2</sub> (aq) + 2H <sub>2</sub> O + 2Ba <sup>++</sup>  | 48.3812        |
| Albite                                       | 1                 | Albite + H <sub>2</sub> O + H <sup>+</sup> = 3SiO <sub>2</sub> (aq) + gibbsite + Na <sup>+</sup>                       | -5.5918        |
| Analcime                                     | 1                 | Analcime + H <sup>+</sup> = 2SiO <sub>2</sub> (aq) + gibbsite + Na <sup>+</sup>  | -0.8967        |
| Anorthite                                    | 1                 | Anorthite + 2H <sub>2</sub> O + 2H <sup>+</sup> = 2SiO <sub>2</sub> (aq) + 2 gibbsite + Ca                             | 12.7159        |
| Beidellite-Ca                                | 1                 | Beidellite-Ca + 2.33H <sub>2</sub> O + 33H <sup>+</sup> = 3.67SiO <sub>2</sub> (aq) + 2.33 gibbsite + Ca <sup>++</sup> | -13.3722       |
| Ca-Al pyroxene                               | 1                 | Ca-Al pyroxene + 2H <sub>2</sub> O + 2H <sup>+</sup> = SiO <sub>2</sub> (aq) + 2 gibbsite + Ca <sup>++</sup>           | 23.0206        |
| Chalcedony                                   | 1                 | Chalcedony = SiO <sub>2</sub> (aq)   | -4.2010        |

composition, temperature, pH and silica concentration in the solution. Various other elements in HLW, occupy positions in the three-dimensional structure, depending upon electronegativity, ionic size and field strength<sup>17</sup>. Na participates easily in the ion-exchange reaction with water<sup>18</sup>; therefore, the normalized mass loss is linked with the rate of release of Na in the solution<sup>19</sup>. The basic strategies for computing chemical equilibrium models in such systems have been reviewed in the literature<sup>20,21</sup>. It is important to understand the behaviour of glass over a long period of time, where newly formed stable mineral species are in equilibrium with the existing conditions. Since chemical composition of waste glass is similar to that of the alumino-silicate minerals observed in the natural environment, the major alteration phases are expected to be the alumino-silicates. Thermodynamic calculations have been used for the prediction of potential alteration phases formed during the long-term disposal periods. These calculations indicate formation of amorphous silica, chalcedony, analcime, smectite, kaolinite, gibbsite or other mineral phases. Also, their formation depends upon the glass composition, solution conditions and reaction progress<sup>22</sup>. Geochemical codes such as EQ3/6 and GWB help to find out the stability of secondary mineral phases for a longer period (~100 years). Hence, discrepancy between the predicted phases and the actually formed min-

eral phases is partly caused by uncertainty in the thermodynamic datasets available with the codes, as the actually formed mineral phases are non-ideal phases. The initial composition of the solution, including all species involved in further reaction was computed. Understanding these calculations is essential as several factors contributing to the nucleation and growth of secondary phases include kinetic constraints on precipitation<sup>23</sup>.

Experiments have been simulated using EQ3/6 software package, which computes distribution of chemical species in an aqueous solution from input major oxide data. It calculates concentration and activity of all the dissolved species for which thermodynamic datasets are available in the database. The saturation state of the fluid is determined with respect to all relevant mineral phases in the database. EQ6 is capable of computing several types of mass transfer models. It utilizes the concept of approximation of irreversible chemical reactions by a series of infinitesimally small increments of reversible reactions. If solution becomes saturated with one or more minerals at any stage of the reaction in progress, a statement of the law of mass action for the corresponding hydrolysis reaction is incorporated in the array of equations<sup>24</sup>. Relative reaction rate of the reactant mineral is specified in the calculations by evaluating at each increment of progress of the reaction using specified values of

**Table 4.** Speciation, activity constant, dissolution equation and saturation index calculated for obsidian glass

| Species/minerals                | Activity constant | Dissolution equation   | log <i>Q/K</i> |
|---------------------------------|-------------------|--|----------------|
| SiO <sub>2</sub> (aq)           | 40.64             | SiO <sub>2</sub> (aq) = SiO <sub>2</sub> (aq)  | 0.0000         |
| H <sub>2</sub> SiO <sub>4</sub> | 14.32             | H <sub>2</sub> SiO <sub>4</sub> + 2H <sup>+</sup> = SiO <sub>2</sub> (aq) + 2H <sub>2</sub> O                            | 24.0746        |
| Beidellite-Ca                   | 1                 | Beidellite-Ca + 2.33H <sub>2</sub> O + 0.33H <sup>+</sup> = 3.67SiO <sub>2</sub> (aq) + 2.33 gibbsite + Ca <sup>++</sup> | -13.3722       |
| Chalcedony                      | 1                 | Chalcedony = SiO <sub>2</sub> (aq)   | -4.2010        |

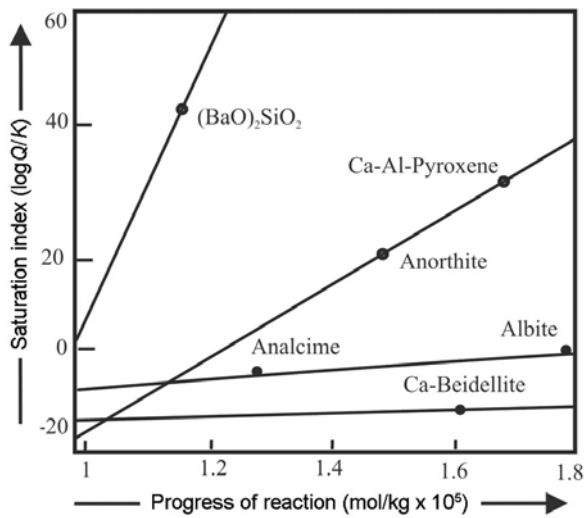


**Figure 2.** Data plots between progress of reaction and saturation index for barium borosilicate (BBS) glass at 300°C in a nearly closed system indicating formation of aluminosilicate mineral phases.

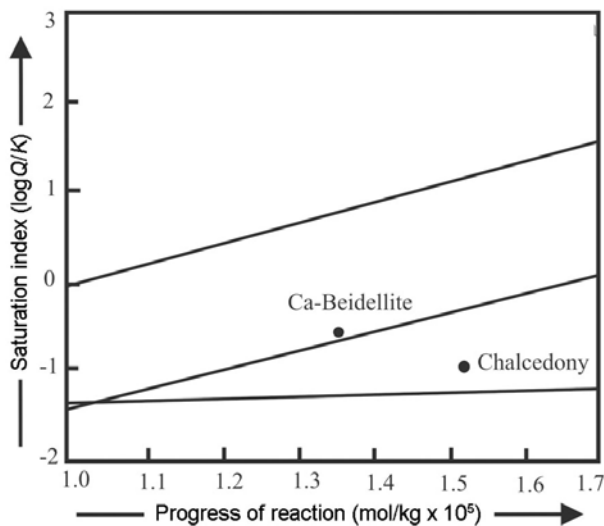


**Figure 3.** Data plots between progress of reaction and saturation index for obsidian glass at 300°C in a nearly closed system indicating formation of aluminosilicate/silicate mineral phases.

the rate constants. The calculations presented were to some extent of a closed system. Product phases remain in equilibrium with the fluid and re-dissolve when the fluid ceases to be saturated with respect to them.

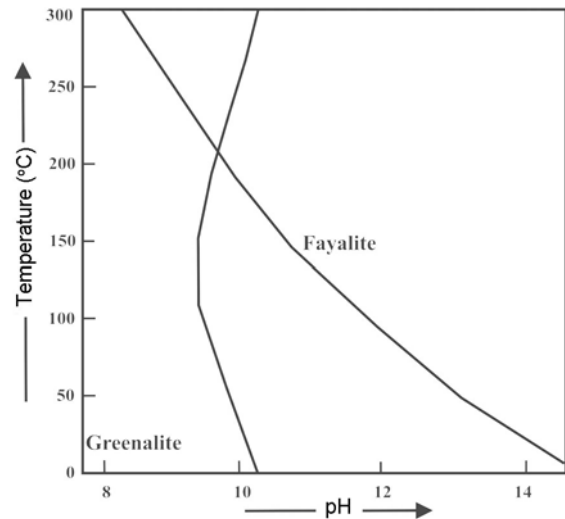


**Figure 4.** Simulated AVS glass data plotted between thermal stability of glass species and their pH values, indicating the appearance of greenalite and fayalite along the curve.

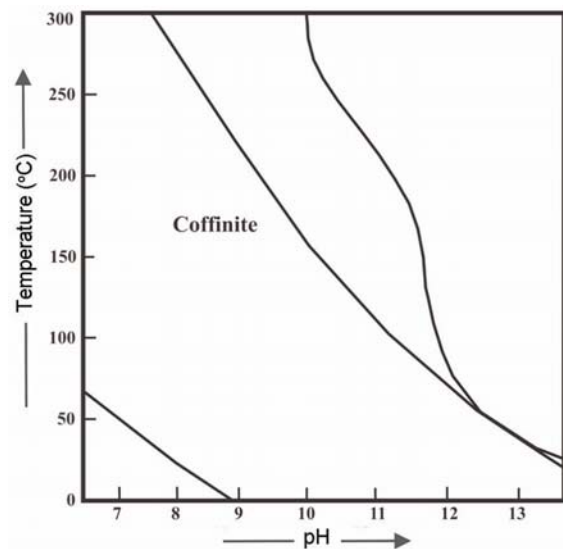


**Figure 5.** Simulated BBS glass data plotted between thermal stability of glass species and their pH values, indicating the appearance of coffinite along the curve.

Dissolution equations for the AVS (Table 2), BBS (Table 3) and obsidian (Table 4) glasses were calculated, and based on these equations, the progress of reaction has been plotted against saturation index (log*Q/K*). These

data plots (Figures 2–4) indicate saturation with respect to solid phases. It has been found that chalcedony and Ca-beidellite are formed when the solution acquires pH of 8.03 at 300°C and a pressure of 1300 psi (refs 10 and 11). The temperature–activity and temperature–fugacity relationships show the effects of temperature on the stability of minerals and predominance of aqueous species in the chemical systems. Thermal stability of glass species versus pH data plots (Figure 5) show the presence of iron-rich minerals leading to the formation of greenalite and fayalite. In BBS glass, presence of coffinite is corroborated when thermal stability of glass species versus pH is plotted (Figure 6). The molar percentage of cationic composition based on major oxide data of obsidian, when simulated, shows the presence of chamosite and beidellite. The EQ3/6 and GWB software and database are suitable for the present study of alteration mechanism in nuclear waste and natural glasses. The calculations presented here are of a nearly closed system, where neo-formed mineral products are in equilibrium with the fluid and they re-dissolve when the fluid ceases to be saturated. Glass data simulation indicates its transformation into secondary phases—quartz, beidellite and illite. Formation of iron-rich fayalite and greenalite is observed in case of AVS, whereas coffinite is formed from the BBS glass.

Behaviour of nuclear waste-loaded and natural glasses shows that after interaction with the environment and formation of neo-formed stable mineral species, they attain equilibrium with the physico-chemical conditions. Results show distribution, concentration and activity of chemical species in an aqueous solution. The mineral phases remain in equilibrium with the fluid and re-dissolve when the fluid ceases to be saturated. The activities and molalities of aqueous species together with the number of moles of each mineral species produced and degenerated

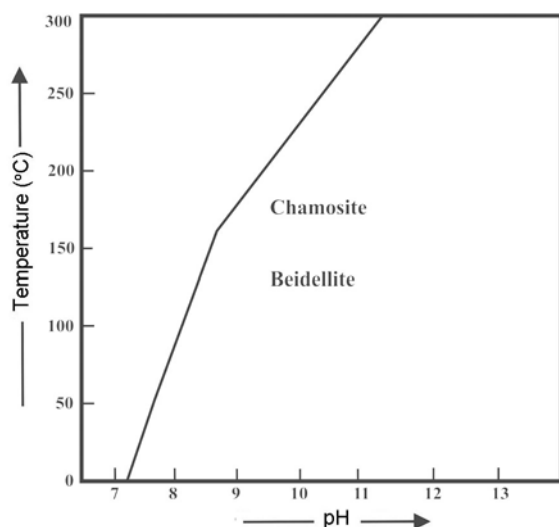


**Figure 6.** Simulated obsidian glass data plotted between thermal stability of glass species and their pH values, indicating the appearance of chamosite and beidellite along the curve.

during the reaction progress (as a function of time) were computed. They show discrepancy between the predicted and actually–formed mineral phases<sup>12</sup>, possibly attributed to uncertainty in the thermodynamic datasets<sup>8</sup> available with geochemical codes because actually mineral phases are formed under non-ideal conditions. Modelling, chemical analysis, laboratory experiments and database are mutually inter-dependent and therefore critically validated<sup>7,10,11,24,25</sup>. However, similar phyllosilicate formation sequences were reported from alteration facies of pillow lavas in the Viviane and Fuchsia drill holes at Mururoa atoll<sup>26</sup>. Alteration mechanism, mineral paragenesis, alteration rate and control of geochemical parameters obtained after chemical reaction modelling by these codes have also been validated by the chemico-mineralogical attributes of the surface layers and alteration products obtained after the laboratory experiments<sup>7,10,11,24,25</sup>. As stated previously<sup>1–3</sup>, the long-term active period in an actual repository is predicted to be of the order of 10<sup>6</sup> years; therefore, the code models must be rigorously investigated to address 10<sup>6</sup> years of geochemical evolution in the repository. In this context, it is worthwhile to mention the recent findings<sup>11,27</sup> that a secondary layer develops over the nuclear waste and natural glass substrates which retains Si, Al, and Mg ions, suggesting its fixation in the alteration products. Moreover, high retention of Ti, Mn and Fe ions implies release of small amounts of these elements into the solution. With the evolution of the secondary layer and retention of less soluble ions, the obstructive effect of the secondary layer increases and the initial release rate diminishes with time. Natural geological features recognized in regard to alteration include devitrification of glass along the cracks, formation of spherulite-like structures and formation of yellowish-brown palagonite, chlorite, calcite, zeolite, and finally white-coloured clays which are commonly associated with the altered obsidian glass. Such obsidian glass and its altered products serve as a standard reference as they have already suffered alteration in the natural environment since their inception (~66 Ma ago)<sup>11,27</sup>. The long-term performance assessment of obsidian glass in natural conditions encompasses the decay period (300–500 years) of Cs and Sr (short-lived isotopes) as well as radioactive decay till ~1 Ma (refs 1–3).

1. Srinivasan, M. and Dingankar, M. V., Long-lived fission reactor waste problem: fact or fiction? *Waste Manage.*, 1992, **12**, 313–322.
2. Dingankar, M. V., Kalyanasundaram, V. and Srinivasan, M. A., Reassessment of long-lived actinide waste hazard potential from Th–<sup>233</sup>U-fueled reactors. *Waste Manage.*, 1992, **12**, 359–372.
3. Hench, L. L., Clark, D. E. and Campbell, J., High level waste immobilization forms nuclear and chemical. *Waste Manage.*, 1984, **5**, 149–173.
4. Shrivastava, J. P., Bajpai R. K. and Rani, N., A review on corrosion mechanism in borosilicate nuclear waste glass for long-term performances assessments in geological repository. *J. Geol. Soc. India*, 2008, **72**, 238–244.